

# Factors Governing Electron Capture by Small Disulfide Loops in Two-Cysteine Peptides

Élise Dumont,\* Pierre-François Loos, and Xavier Assfeld

Équipe de Chimie et Biochimie Théoriques, UMR 7565 CNRS-UHP, Institut Jean Barriol, (FR CNRS 2843),  
Faculté des Sciences et Techniques, Nancy-Université, B.P. 239, 54506 Vandoeuvre-lès-Nancy, France

Received: July 22, 2008

Integrated molecular orbital–molecular orbital (IMOMO) calculations on 17 short disulfide-bridged peptides (up to 16 residues, with at most five intraloop residues) were performed to elucidate some factors controlling their electron capture. These illustrative systems display contrasted behaviors, shedding light on several criteria of differentiation: size, shape, and rigidity of the disulfide-linking loop, intramolecular hydrogen bonds, etc. The geometrical malleability of disulfide radical anions, whose existence and role as intermediate have been evidenced, is discussed. The disulfide elongation (by ca. 0.7 Å) upon electron capture induces “soft” structural damages for these turn structures, with a weakening or cleavage of vicinal hydrogen bond(s). On the basis of a series of six Cys-Ala<sub>n</sub>-Cys peptides, it is proposed that electron affinity reflects the topological frustration of these short and highly constrained structures. Results for a series of amino acid mutations are analyzed for the Cys-Xxx-Yyy-Cys motif, common to redox enzymes of the thioredoxin superfamily.

## I. Introduction

Formation of disulfide linkages by association of two spatially close cysteines has been early recognized as a fundamental driving force in protein folding,<sup>1,2</sup> along with stabilizing hydrogen bonds between residues. A key specificity of the sulfur–sulfur bond is an intermediate strength between weak interactions (van der Waals, hydrogen bonds, etc.) and typical covalent bonds. For instance, the dissociation energy of the disulfide linkage is close to 65 kcal/mol.<sup>3</sup>

On the one hand, they are strong enough to induce and maintain a protein fold: in cyclotides, the subtle layout of three disulfide bonds leads to a remarkable stabilization (cystine knot).<sup>4</sup> In a synthesis context, closure of macrocycles<sup>5,6</sup> or nanotube-like structures<sup>7,8</sup> as ensured by disulfide bond is a newly developed and promising option. On the other hand, any modification of the surroundings (oxidative stress, chemical reactant, or mechanical force) is likely to affect in first place disulfide bonds.

This remarkable versatility is at the heart of the thiolate–disulfide exchange and also constitutes a key asset for designing ingenious applications. Cleavage of the disulfide bond can be used to controllably zip and unzip a macrocycle (e.g., thia zip reaction)<sup>9</sup> or as a trigger to monitor unfolding of small peptides.<sup>10</sup> Their chemical flexibility also confers to sulfur-containing species a special importance as ligands (thiolate) in organometallic synthesis.<sup>11–13</sup>

Yet, we may still lack an exhaustive overview of the wide range of reactions that can undergo a disulfide linkage. Joint experimental and theoretical studies established that simple aliphatic or aromatic disulfides can fix one electron, forming a symmetric radical anion.<sup>14–16</sup> The covalent sulfur–sulfur bond is significantly elongated during the process, typically by 0.7 Å, but *not* cleaved. Its dissociation is disfavored, with products lying higher in energy (roughly 24 kcal/mol for gas phase dimethyl disulfide). Such systems have been qualified as hemibonded in the 1950s,<sup>17</sup> which was later confirmed by topological analysis.<sup>18</sup> This one-electron capture (indirectly

induced by X-ray irradiation or reducing agents constitutes an intriguing reaction. It is of first importance to understand in depth this conceptually very simple chemical reaction, which can be viewed as a prototype. It has been shown that resulting disulfide radical anions can either be stable<sup>19</sup> or of transient nature, leading to electron capture dissociation (ECD) for multiply charged proteins.<sup>20–22</sup> Their existence in biological systems has been early recognized with flash photolysis<sup>23</sup> and pulsed radiolysis.<sup>24–26</sup> Recently, Weik et al. reported time-resolved measurements of structural damage induced by synchrotron radiation.<sup>27</sup> The authors provide Fourier maps showing elongation for each of the three disulfide linkages, which is characteristic of radical anion species. Interatomic sulfur distances were found to be roughly equal to 2.7 Å, which is similar to aliphatic systems, none of them being dissociated. The latter was confirmed shortly after by *ab initio* calculations.<sup>28,29</sup> By establishing the *specific* attachment to disulfide linkages, this breakthrough, seminal work has initiated many exciting and interconnected questions. For instance, two very recent studies by Rauk and co-workers have aimed to elucidate the outcome of this so-formed, long-lifetime (ca. 1 s) intermediate in its very own biological environment (thioredoxin).<sup>30,31</sup> Many aspects of the formation of disulfide radical anions also remain answerless:

1. How can the structure and environment of biological disulfide radical anions lead to a differentiation with respect to aliphatic analogues (in terms of stability, geometry, and ease of formation)?

2. What structural damages are caused by electron addition on a disulfide linkage?

3. How tunable is a disulfide linkage in a biological environment? Can we identify key factors governing disulfide reducible properties? What is the effect of an amino acid mutation?

Our main motivation for performing this study was to collect first elements of answer for this series of questions. We recently investigated electron capture by cyclic aliphatic disulfides and evidenced the key role of the dihedral angle  $\tau(\text{C}-\text{S}-\text{S}-\text{C})$ .<sup>32</sup> It can be expected that electron capture in biological systems will differ in many regards. The next

\* Corresponding author. E-mail: Elise.Dumont@cbt.uhp-nancy.fr.



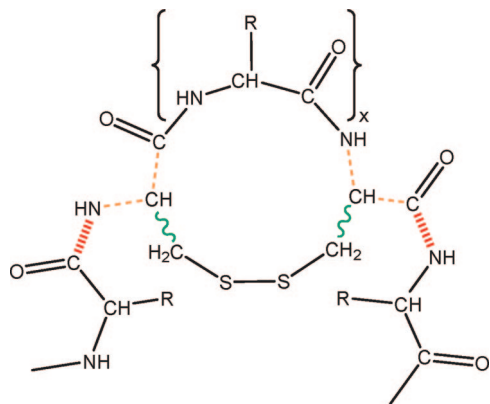
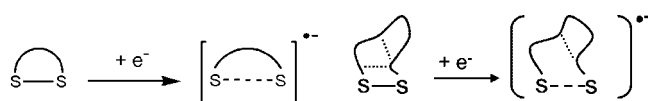


**Figure 1.** Representation of the (three) possibilities for defining a hybrid QM/MM or QM/QM' frontier.  $x$  denotes the number of intraloop residues.  $R$  denotes the side chain of the residues. Wavy lines denote the C–C bonds which have been defined as QM/MM frontiers in this work.



(a) Organic disulfide: the prototype for an aliphatic arc is a  $(CH_2)_n$  chain. (b) Biological system: the arc is a short amino acid chain.

**Figure 2.** Schematic representation of the one-electron addition on (i) aliphatic cyclic disulfides vs (ii) short disulfide-bridged peptides. The sulfur–sulfur hemibond in the radical anion is represented with a dashed line. Intraloop hydrogen bonds are denoted with light dashed lines: they do not contribute to the overall structure of the turn.

frontiers, two of the bonds (C–N) being polarized (they are displayed with dashed lines in Figure 1) or (ii) to impose the frontier on the peptidic bonds (front line). Because of their polarity and  $\pi$ -delocalization, they are intrinsically highly delicate to properly partitioned.<sup>90</sup> This inevitably leads to dramatic errors within a link-atom scheme.<sup>56</sup>

Effects of a carbon–carbon cut were recently assessed by Bergès et al. in a similar context.<sup>29</sup> They conclude that a “relatively restrained QM part seems to be sufficient for modeling [disulfide radical anions] electronic property”, thus comforting us in our choice. This probably reflects the highly localized character of the disulfide bond density. An additional benefit of a proximal cut is to limit the size of the QM part, which needs to be treated with a high level of theory (MP2/6-31+G\*\*). The choice for this basis set is based on previous benchmark calculations on dimethyl disulfide.<sup>32</sup> They were performed to investigate the basis set convergence for adiabatic electron affinities ( $EA_{ad}$ ) and is proven to give meaningful results.<sup>57</sup> While geometrical parameters are correctly reproduced as soon as the basis set is large enough and includes diffuse functions, electron affinities are much slower to converge. We found that a solid compromise consists in using the Pople basis set 6-31+G\*\*, which gives a value for electron affinity close to the exact value (ca. +0.10 eV).<sup>58</sup>

Benchmark calculations on DEDS were performed to choose the most appropriate level of theory for the QM' part (Table 1). It can be checked that the QM/QM' partitioning does not induce serious artifacts on geometries, whatever HF or DFT methods are used. Estimation of absolute adiabatic attachment energies ( $EA_{ad}$ ) is more problematic. The best agreement between QM/QM' calculations and the experimental values of 0.05–0.10 eV<sup>14</sup> is obtained when the nonhybrid BLYP functional is used to treat the QM' part.<sup>59,60</sup> Yet, this improvement

would come at the price of much more expensive, resource-demanding calculations. The Hartree–Fock method appears as the best compromise, given that we are interested in *relative* energies ( $\Delta EA_{ad}$ ). Auxiliary calculations established that the latter are much more stable with respect to the level of theory. Systems will therefore be described with a coupled MP2/6-31+G\*\*: $HF/6-31G^*$  scheme, as implemented within the Gaussian 03 series of programs.<sup>61</sup>  $\langle S^2 \rangle$  values were never greater than 0.77 (to be compared to the exact value of 0.75), such that no contamination spin effect will affect our results.

Tetrapeptides, as listed in Table 2, for which experimental structures are not available, were generated using Molden,<sup>62</sup> taking characteristic angles of  $\beta$ -turn classification.<sup>63</sup> We then selected the energy minimum, as calculated with the PM3MM method: this procedure is inspired by an earlier study by Mohle et al.<sup>64</sup> As expected, most minima were found to be of types  $\beta I$  and  $\beta I'$ . For bigger peptides, we generated Ramachandran plots (CHARMM force field) to select the lowest energy conformer: this ensures us to start up with a reasonable structure, although the definitive determination of 3D structure is not manageable. Full ab initio geometry optimizations were then performed from these starting points. Final geometrical parameters are given in angstroms and degrees. Rmsd values between neutral and anionic forms were computed following the method of Kabsch<sup>65</sup> as implemented in the VMD software<sup>66</sup>—hydrogen atoms were excluded.

### III. Results and Discussion

**A. Description of the Panel: A Family of Peptides.** Very short disulfide-linked peptides ( $m$ -mers, where  $m$  denotes the total number of residues) differ by many factors from organic compounds, as schematized in Figure 2. The first characteristic is the number  $n$  of intraloop residues.<sup>91</sup> Peptidic bonds locally impose a quasi-planarity, thus breaking the isotropy of the arc with a change of its shape and rigidity. The most natural choice for building up a representative panel is to consider peptides of general formula Cys-Xxx $_n$ -Cys-. Six peptides with Xxx taken as L-alanine are considered, which enables a comparison with experimental results.<sup>67</sup> To enlarge this set, other disulfide-containing peptides were gathered from structures available in the literature, either designed or naturally occurring. Their names and sequences are listed in Table 2, and optimized geometries are displayed in Figures 3 and 4 for neutral and radical anionic species, respectively. Diethyl disulfide (DEDS) was taken as an organic, ring-free compound for calculations of relative adiabatic electron affinities ( $\Delta EA_{ad}$ ).

For cyclic peptides in our set, the choice of capping groups is bypassed. For synthetic compounds, we simply kept C- and N-terminal protecting groups. They will most often be respectively -NHMe and -Boc, as obtained via the widely used Boc (*tert*-butyloxycarbonyl) synthesis protocols. In addition to the naturally occurring amino acids, two uncoded ones are considered. 2-Aminoisobutyryl acid (Aib) is commonly used in synthesis instead of alanine or glycine, as it tends to stabilize  $\alpha$ -helices. Another uncoded amino acid is penicillamine (Pen), corresponding to a cysteine residue where  $C_{\beta}H_2$  have been formally replaced by  $C_{\beta}(CH_3)_2$ . In the rest of the paper, conventional three-letter codes for  $\alpha$ -amino acids will be used.

A potential source of difficulty is the partial loss of secondary structure upon (gas-phase) optimization, as can be observed for labile structures. Our systems were chosen to have well-defined conformations, and it was checked that they are maintained. For this reason, only the structure (II) of oxytocin was considered<sup>68,69</sup> (PDB ID 1XY2).

**TABLE 2: Geometries and Electron Affinity for One-Electron Addition on Small Peptides Containing a Disulfide Linkage—neutral and Associated Radical Anions—Represented in Figures 3 and 4<sup>a</sup>**

compound	<i>m</i>	<i>(n, n')</i>	structure				electron affinity		
			<i>d</i> (S–S)	$\angle$ (S–S–C)	$\tau$ (C–S–S–C)	<i>d</i> <sub>HB</sub>	EA <sub>ad</sub>	$\Delta$ EA <sub>ad</sub>	rmsd
Cys-Cys motif									
NHMe-Cys-Cys-Boc ( <b>0a</b> )	2	(0,6)	2.07	105.7, 106.1	98.6				
			2.94	90.6, 95.5	102.8				
malformin A ( <b>1</b> ) <sup>84–87</sup>	5	(0,6)	2.07	106.4, 106.7	97.9		+0.54 (–0.10)	+0.97	0.177
cyclo-D-Cys-D-Cys-L-Val-D-Leu-L-Ile helix ( <b>2</b> )	16	(0,6)	3.19	96.5, 100.2	91.1		+0.70 (–0.22)	+1.13	0.474
Cys-Gly <sub>14</sub> -Cys			2.07	105.6, 108.9	65.5				
			2.89	97.3, 106.6	47.5		+0.59 (–0.01)	+1.02	1.697
Cys-X-Cys motif									
Cys-Ala-Cys ( <b>0b</b> )	3	(1,9)	2.09	104.3, 102.2	–142.2				
			2.84	86.0, 105.3	–164.0		+1.06 (+0.17)	+1.49	1.068
Cys-X <sub>2</sub> -Cys motif									
Cys-Ala-Ala-Cys ( <b>0c</b> )	4	(2,12)	2.06	101.8, 101.7	–83.8	2.19			
			2.80	88.7, 88.8	–83.0	2.20	+0.41 (–0.01)	+0.84	0.257
Cys-Pro-Aib-Cys ( <b>3a</b> ) <sup>34</sup>	4	(2,12)	2.05	104.7, 104.8	–103.3	2.13			
			2.75	94.5, 98.9	–106.4	2.29	+0.40 (0.00)	+0.83	0.261
Cys-Pro-Phe-Cys ( <b>3b</b> ) <sup>34</sup>	4	(2,12)	2.06	102.5, 104.4	–109.3				
			2.73	89.0, 95.0	–118.2		+0.53 (0.00)	+0.96	0.587
Cys-Pro-Gly-Cys ( <b>3c</b> )	4	(2,12)	2.05	104.6, 104.2	–104.2	2.20			
			2.73	93.9, 88.2	–122.6	2.65	+0.53 (+0.03)	+0.96	3.483
Pen-Pro-Aib-Cys ( <b>3d</b> )	4	(2,12)	2.05	105.1, 109.9	–105.0	2.38			
			2.77	101.4, 110.9	–112.5	2.91	+0.53 (+0.08)	+0.96	0.516
Cys-Pro-Aib-Pen ( <b>3e</b> )	4	(2,12)	2.05	109.4, 105.6	–103.6	2.10			
			2.81	96.1, 111.9	–102.5	2.20	+0.44 (+0.07)	+0.87	0.580
Pen-Pro-Aib-Pen ( <b>3f</b> )	4	(2,12)	2.05	110.9, 109.9	–112.8	2.21			
			2.87	114.2, 111.5	–107.6	2.59	+0.57 (+0.20)	+1.00	1.565
Cys-Phe-Gly-Cys-Gly ( <b>3g</b> ) <sup>88</sup>	5	(2,12)	2.06	104.4, 102.3	–78.2	2.18			
			2.85	88.4, 96.6	–66.8	2.62	+0.62 (–0.10)	+1.05	0.502
Cys-X <sub>3</sub> -Cys motif									
Cys-Ala-Ala-Ala-Cys ( <b>0d</b> )	5	(3,15)	2.07	101.5, 103.4	–120.5	1.99			
			2.83	91.0, 94.5	–135.4	1.99	+0.72 (+0.03)	+1.15	0.310
Cys-X <sub>4</sub> -Cys motif									
Cys-Ala <sub>4</sub> -Cys ( <b>0e</b> )	6	(4,18)	2.06	101.1, 101.8	–73.2	2.60			
			2.85	88.3, 90.0	–85.1		+0.38 (–0.09)	+0.81	0.542
hairpin ( <b>4</b> ) <sup>73</sup>	6	(4,18)	2.06	100.5, 105.1	–90.7	2.16, 2.29			
Boc-Cys-Val-Aib-Ala-Leu-Cys-NHMe oxytocin ( <b>5</b> ) <sup>68,69</sup>	9	(4,18)	2.09	108.5, 103.4	–102.9	2.66			
			2.80	103.3, 119.2	–61.1	2.37	+0.76 (–0.14)	+1.19	1.941
Cys-Tyr-Phe-Glu-Asp-Cys-Pro-Arg-Gly									
Cys-X <sub>5</sub> -Cys motif									
Cys-Ala <sub>5</sub> -Cys ( <b>0f</b> )	7	(5,21)	2.06	106.8, 108.0	–97.7	2.28			
			2.80	87.7, 108.7	–97.8	2.04	+0.65 (–0.06)	+1.08	0.402
aliphatic disulfides									
DEDS		– (→∞, →∞)	2.06	102.1	–85.3				
		– (→∞, →∞)	2.78	89.0	–87.3		–0.43 (–0.09)	+0.00	0.326
1,2-dithiooctane		– (–, 6)	2.06	103.2, 104.3	96.1				
		– (–, 6)	2.79	93.5, 97.2	98.8		–0.41 (–0.05)	+0.02	0.090

<sup>a</sup> Calculations were performed at the MP2/6-31+G\*\* level of theory. *d*<sub>HB</sub> refers to intraloop hydrogen bonds (when existing). Adiabatic electron attachment energies, absolute EA<sub>ad</sub> and relative  $\Delta$ EA<sub>ad</sub>, are given in eV; values in parentheses correspond to electron affinity limited to the high-level system (–CH<sub>2</sub>–S–S–CH<sub>2</sub>). *m* corresponds to the total number of residues for a given peptide and *n* to the number of residues forming the Cys-Cys loop. Alternatively, *n'* denotes the number of atoms of the arc.

**B. Versatile Geometry of Biological Disulfide Radical Anions.** The key feature of disulfide one-electron addition is a drastic elongation of the covalent disulfide bond. We found it to be decisive for intramolecular biological disulfides, as the lengthening occurs in a cycle. Our results gathered in Table 2 and establish the following:

1. The dissociation of the radical anion is never observed, with a nature of hemibond confirmed by atomic spin densities close to 0.5 on each sulfur atom. Short loops easily accommodate the drastic lengthening of disulfide linkage.

2. A wide range of intersulfur distances for anionic species is obtained: their values are comprised between 2.73 and 3.19

Å respectively for (**3b**, **3c**, **4**) and (**1**), compared to 2.78 Å for DEDS. Elongation of the hemibond can be either reduced or amplified.<sup>92</sup> For neutral disulfides, variations are much more limited, with distances comprised between 2.05 and 2.09 Å.

3. Similarly, the dihedral angle  $\tau$ (C–S–S–C) for hemibonded systems is comprised between –61.1° and –164.0° (compared to –87.3° for DEDS).

This remarkable malleability of hemibonded disulfide linkage can be further commented on a simple model, i.e., diethyl disulfide. The dissociation curve for the radical anion is extremely flat (Figure 1 in the Supporting Information), such that no clear upper limit can be inferred for a three-electron

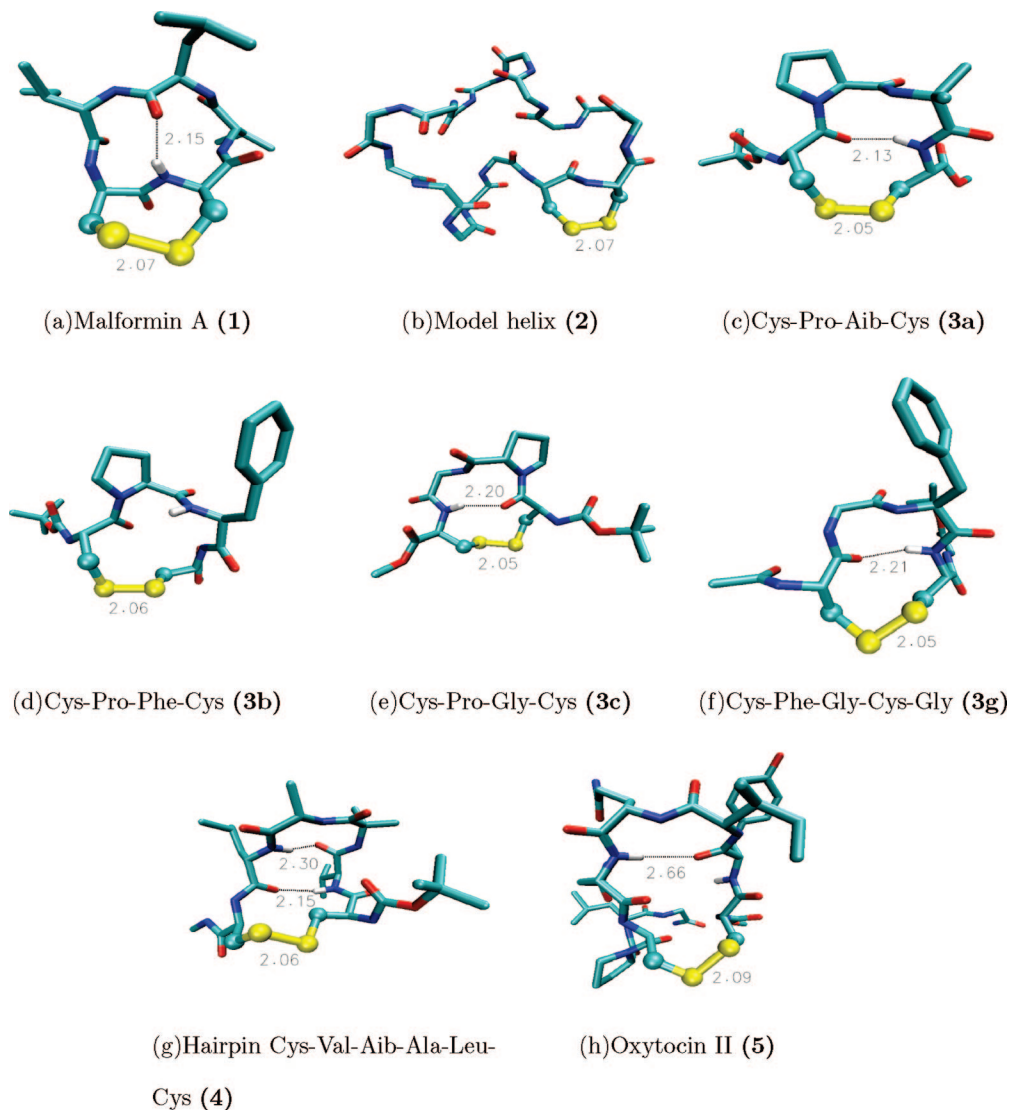


**Figure 3.** Optimized MP2/6-31+G\*\*/HF/6-31G\* structures for neutral structures. The high-level QM part is depicted with balls, while the low-level structure is represented with sticks (backbone and side chain). Sulfur–sulfur distance and hydrogen bonds, when existing, are given in Å. Labels refers to Table 2.

two-sulfur distance. Our calculations show that a ring effect of 3 kcal/mol suffices to induce a compression up to ca. 2.4 Å, or conversely an elongation up to ca. 3.2 Å. Similarly, torsion profiles also are considerably weakened upon electron capture.<sup>32</sup> Thus, any conformational preference of the loop (either cyclic skeleton or backbone) is immediately reflected on SS distances of disulfide radical anions.

**C. Evolution of Peptide Structure upon Disulfide Electron Capture.** Disulfide elongation inevitably induces a geometrical reorganization of the peptide. The associated structural damage is a crucial aspect of radiation damage. Our results suggest some preliminary features by comparing evolution of geometries upon electron capture, which are displayed in Figures 3 and 4. In most situations, the overall transformation tends to be soft. Effects of disulfide elongation remain limited to the following: (i) Weakening or cleavage of one or several proximal hydrogen bond(s), when existing. This is for instance exemplified by the tetrapeptide **3c**, whose intraloop HB is significantly elongated (2.20 to 2.65 Å). (ii) The eventual formation of new hydrogen bonds, as observed for peptides **4** and **5**. When considering such short peptides, “structural damage” may be an irrelevant and perhaps misleading term because they do not have a proper secondary structure, like proteins. In fact, the closure of the

$\beta$ -turn by a disulfide clamp gives rise to an important topological frustration. This aspect turns out to be crucial for understanding energetic aspects of electron addition on small disulfide loops, which are considered in the next subsection.

**D. Factors Governing Electron Affinity.** Values for the adiabatic electron affinity (both absolute and relative to DEES) are reported in Table 2. More than a crude number, they reflect the ease by which neutral disulfides can form a radical anionic species. For the sake of clarity, we first limit the discussion to the six peptides of the series Cys-Ala<sub>n</sub>-Cys.

**1. Cys-Ala<sub>n</sub>-Cys Peptides: A Relation between Electron Affinity and Conformational Strain.** Relative electron affinities  $\Delta E_{ad}$  for the Cys-Ala<sub>n</sub>-Cys series of peptides are strongly positive, with values ranging from +0.81 to +1.49 eV. Their variation as a function of  $n$  is nonmonotonous. It is remarkable that peptides with even values of  $n$  are found to be less reactive toward one-electron addition, with the following order: 4, 2, 0, 5, 3, and 1. Let us note that it corresponds globally to the natural propensity of Cys-Xxx<sub>n</sub>-Cys motif in proteins,<sup>67</sup> where even residue number cycles are most often encountered.

In addition to these statistics, both theoretical studies on peptide cyclizations<sup>70</sup> and kinetic measurements on redox processes<sup>67</sup> have brought further evidence for this dependence

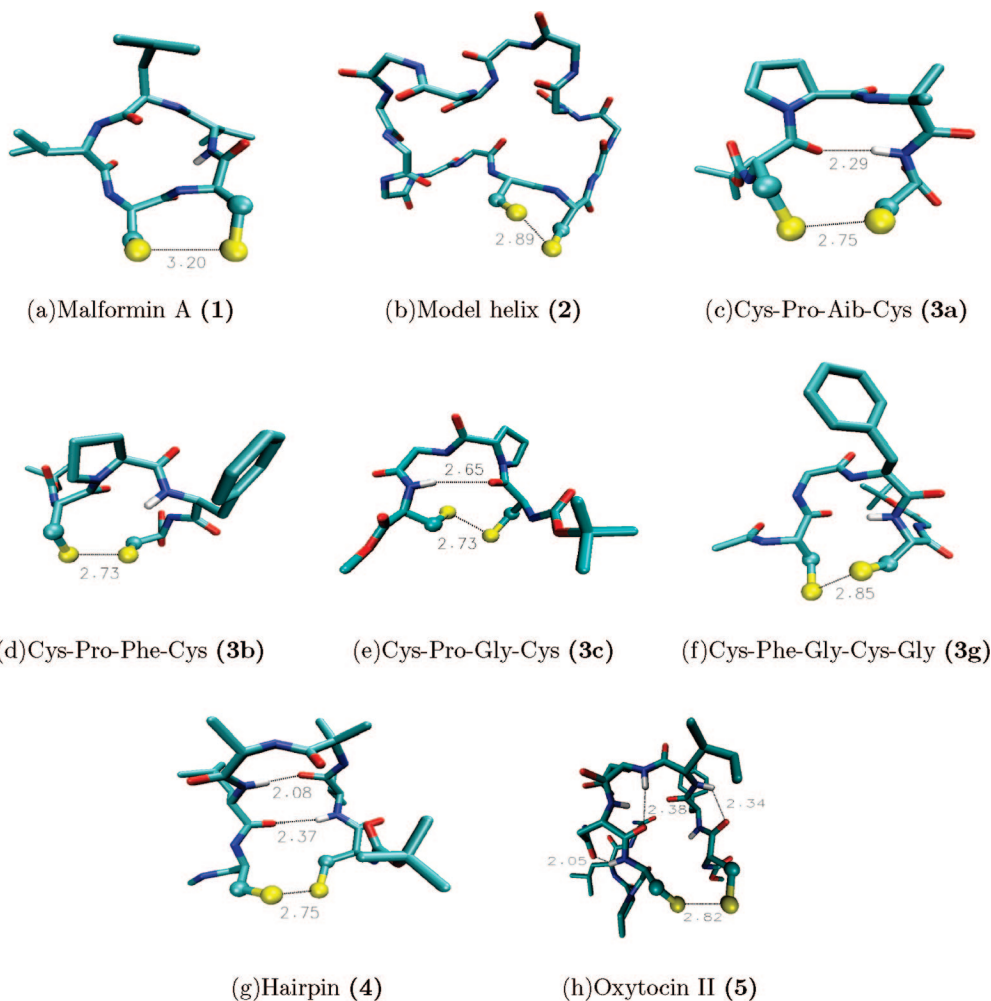


**Figure 4.** Optimized MP2/6-31+G\*\*/HF/6-31G\* structures for radical anion structures. The high-level QM part is depicted with balls, while the low-level structure is represented with sticks (backbone and side chain). Sulfur–sulfur distance and hydrogen bonds, when existing, are given in Å. Labels refers to Table 2.

on the odd–even nature of  $n$ . They all agree that short cyclic peptides with odd values of  $n$  are more reactive in a general way. The latter study by Zhang and Snyder reports rate constants for the formation and opening of a series of small disulfide-linked peptides.<sup>67,93</sup> The ratio  $K_c$  of these two rate constants  $k_c$  and  $k_o$  is proposed as a measure of the conformational strain.

$$K_c = \frac{k_c}{k_o} \quad (1)$$

It provides a more quantitative assessment of the ease of closure for these peptides. A close agreement between rank orders for  $\log K_c$  (2, 4, 5, 0, 3, and 1) and for our calculated adiabatic electron affinities  $\Delta EA_{ad}$  is found. A linear relation is obtained (Figure 5,  $N = 6$ ,  $R^2 = 0.952$ ). We recently reported an analogue relation for a series of 1,2-dithiacycloalkanes, whose electron affinity was found to vary linearly with the ring strain energy ( $N = 7$ ,  $R^2 = 0.971$ ).<sup>32</sup> Taken together, these results strongly suggest that the topological frustration of a disulfide-linked compound is a key factor determining its electron affinity: the more constrained the neutral system, the higher its electron affinity.

**2. DFT Functionals Performance for Reproducing Relative Electron Affinities of Disulfide Linkages.** Systematic failings of DFT for describing two-center three-electron bonds have been

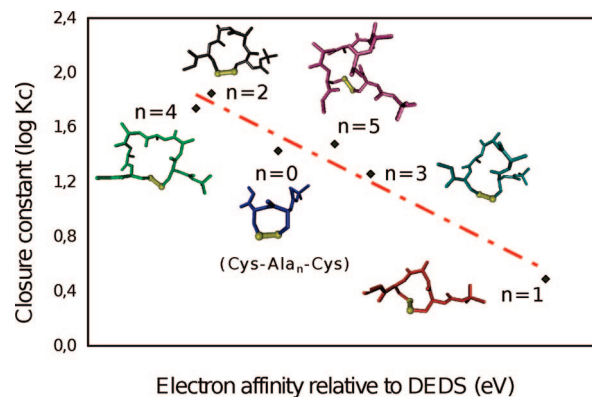


**Figure 5.** Relationship between  $\log K_c$ , taken from ref 67, and electron affinities  $\Delta EA_{ad}$  relative to DEDS for a series of peptides -Cys-Ala $_n$ -Cys- ( $N = 6$ ,  $R^2 = 0.952$ ).

studied on model systems and in depth rationalized (cf. section II and references therein). Density-based calculations may nevertheless reproduce trends which we are precisely interested in.<sup>94</sup> Hence, additional QM calculations on the Cys-Ala $_n$ -Cys series of peptides with the nonhybrid BLYP and the hybrid BH&HLYP<sup>71</sup> functionals were performed as a first test. The latter has been shown to perform slightly better for three-electron two-center systems than pure DFT methods.<sup>72</sup> A mixed basis set (6-31+G\*\* for the  $-\text{CH}_2-\text{S}-\text{S}-\text{CH}_2-$  fragment and

6-31G\* elsewhere) was chosen for the sake of consistency with our ONIOM calculations.

Geometrical parameters for the sulfur–sulfur (hemi)bond are given in Table 1 of the Supporting Information. The hybrid BH&HLYP functional is found to give geometries in closer agreement with MP2 calculations, which has been previously reported on model systems.<sup>72</sup> Adiabatic electron affinities  $EA_{ad}$  are systematically higher than the quantities obtained within our QM/QM' approach, by 0.5 eV in mean, which is a signature of self-interaction error.<sup>72</sup> This increment is not constant along the Cys-Ala<sub>n</sub>-Cys series (last column of Table 1, Supporting Information). Consequently, the odd–even dependence is no longer verified for the BH&HLYP functional, with the following rank order: 4, 3, 0, 5, 2, 1. With the nonhybrid functional BLYP, another rank order is found (4, 0, 2, 5, 3, 1), in better agreement with both log  $K_c$  and the MP2/6-31+G\*:HF/6-31G\* level of theory. Quantitatively, the linear relation is no longer observed (see Table 1, Supporting Information). The important scattering arises mostly for the three smallest peptides  $n = 0, 1, 2$ . These results indicate that DFT errors are likely to be *nonsystematic*, and its use should probably be hindered even for relative purposes.

**3. Mutations on Tetrapeptides: The Cys-Xxx-Yyy-Cys Motif.** While the loop length  $n$  turns out to be a key variable for understanding disulfide electron affinity, it is also legitimate to consider effects of amino acids mutations, on either cysteine (direct) or intraloop (indirect) residues. To this end, we chose to focus on the Cys-Xxx-Yyy-Cys tetrapeptides because of their importance as active site for the thioredoxins superfamily of redox enzymes.

Starting from the structure **3a**, direct mutations of one or both cysteinyl residues (Cys → Pen) generate three peptides (**3d–3f**). Optimized geometries for neutral and anionic species are given in Figures 2 and 3 of the Supporting Information. Geometries of the –CH<sub>2</sub>–S–S–CH<sub>2</sub>– neutral fragment are mostly affected by the dihedral angle, with a maximal variation of 10°. The anionic system appears to be more malleable, with a sulfur–sulfur distance lengthened up to 0.12 Å. Electron affinity is systematically enhanced by this mutation, by up to +0.17 eV when both cysteines are mutated. On this particular example, it can be noted that the energetic increments appear to follow a simple addition rule, as mutations on Cys<sub>1</sub> and Cys<sub>2</sub> respectively account for +0.13 and +0.04 eV.

To discuss indirect mutations, we chose to focus on the Cys-Xxx-Yyy-Cys tetrapeptides because of their biological relevance. Mutations of the inner dipeptide -Xxx-Yyy- is known to tune disulfide-linkage reactivity and has been a widely studied motif in the literature.<sup>10,34,73,74</sup> Yet, the way by which the sequence -Xxx-Yyy- controls the redox potential of thioredoxins<sup>75</sup> is not understood. We have considered mutations representative of enzymes of this superfamily: Xxx → Pro, Phe and Yyy → Aib, Phe, Gly. This corresponds to a series of five tetrapeptides, with the subset (**3a**)–(**3c**), (**3g**), and (**0c**), which serves as a reference (Xxx, Yyy = Ala).

Electron affinities  $\Delta EA_{ad}$  for these five peptides range from +0.83 to +1.05 eV respectively for (**3a**) and (**3g**), which corresponds to a narrow range of 0.22 eV. Our results show that proline tends to increase electron affinity of the disulfide linkage ((**3a**)–(**3c**)). This may come from the higher rigidity of the  $\beta$ -turn.<sup>34,76</sup> An exception is found for (**3a**), whose electron affinity is almost equal to the reference Cys-Ala-Ala-Cys (**0c**). Kolano and co-workers have recently highlighted the existence of an intraloop hydrogen bond for this tetrapeptide.<sup>34</sup> The latter

is cleaved upon disulfide electron capture and the concomitant elongation of the linkage (cf. Figure 3c). It slightly counteracts the electron capture, with electron affinities of (**3a**) and (**3b**) differing by 0.13 eV. This value corresponds to the weakening of an hydrogen bond (ca. 3 kcal/mol).

Insertion of an aromatic residue (here Phe) appears to enhance electron affinity for the two tetrapeptides ((**3b**) and (**3g**)). This trend would need to be ascertained and properly traced back on a larger set, as the presence of an aromatic residue in the Cys-Xxx-Yyy-Cys active site has proved to be essential for difference of reactivity between glutaredoxins and thioredoxins.<sup>77</sup>

**4. Trends in the Rest of the Panel.** As the number of intraloop residues  $n$  increases, a greater spread of electron affinities is observed. Relative values range from –0.27 to +1.19 eV (respectively for hairpin (**4**) and oxytocin (**5**)), in spite of the same number of intraloop residues ( $n = 4$ ). It has been early recognized that disulfide reactivity varies in an important way,<sup>78</sup> and not surprisingly, we found a similar conclusion for the one-electron addition.

Oxytocin (**5**) exemplifies how outer-loop residues can modulate the disulfide-linkage electron uptake. This labile structure<sup>68,69,79</sup> is found to undergo an important reorganization upon disulfide elongation (Figures 3h and 4h). It takes advantage of the hemibond malleability to force a dihedral compression (–61.1°) and form an outside HB network in the second  $\beta$ -turn. This driving force could be at the origin of the high value of  $\Delta EA_{ad}$  (+1.19 eV).

By contrast, one-electron addition for one peptide in our set, namely (**4**), is disfavored compared to diethyl disulfide. This designed hairpin<sup>95</sup> is the sole to present a proper secondary structure.<sup>73</sup> Hence, there is no conformational strain to be released, and the disulfide-linkage elongation imposes a geometrical deformation that is globally energetically disfavored. This may be representative of the situation in bigger peptides or proteins because they are products of a many-complicated folding process that ensures a near-optimal release of topological frustration.<sup>80</sup>

#### IV. Concluding Remarks

In this work, a systematic study of one-electron addition on short disulfide-linked peptides is presented. Their structures rely mostly on a disulfide clamp, conferring to such moieties a specific reactivity, in particular toward one-electron addition. The latter is strongly favored, since it tends to eliminate the topological frustration associated with ring closure. Electron affinities are also modulated by amino acid mutation.

Other factors come into play in larger biomolecules, like the presence of charged residues in the vicinity of the disulfide linkage<sup>31</sup> or the characteristic motifs of secondary structure.<sup>57</sup>

**Acknowledgment.** This work was supported by computer resources of the University of Nancy I, France.

**Supporting Information Available:** Potential energy profiles of diethyl sulfide (Figure 1), optimized MP2/6-31+G\*\*:  
HF/6-31G\* structures for neutral (Figure 2) and radical anion (Figure 3) structures, table showing assessment of two DFT functionals performance for describing electron capture by Cys-(Ala<sub>n</sub>)-Cys disulfide-linked peptides (Table 1), and table showing results of linear regression between DFT  $EA_{ad}$  and log  $K_c$  (Table 2). This material is available free of charge via the Internet at <http://pubs.acs.org>.

## References and Notes

- Oas, T. G.; Kim, P. S. *Nature (London)* **1988**, *336*, 42–48.
- Raines, R. T. *Chem. Rev.* **1998**, *98*, 1045–1065.
- Nicovich, J. M.; Kreutter, K. D.; Vandijk, C. A.; Wine, P. H. *J. Phys. Chem.* **1992**, *96*, 2518–2528.
- Daly, N. L.; Clark, R. J.; Craik, D. J. *J. Biol. Chem.* **2003**, *278*, 6314–6322.
- Otto, S.; Furlan, R. L. E.; Sanders, J. K. M. *Science* **2003**, *297*, 590–593.
- Nabeshima, T.; Nishida, D.; Saiki, T. *Tetrahedron* **2003**, *59*, 639–647.
- Lu, H. S. M.; Volk, M.; Kholodenko, Y.; Gooding, E.; Hochstrasser, R. M.; Degradó, W. F. *J. Am. Chem. Soc.* **1997**, *119*, 7173–7180.
- Wong Shi Kam, N.; Liu, Z.; Dai, H. J. *Am. Chem. Soc.* **2005**, *127*, 12492–12493.
- Tam, J. P.; Lu, Y.-A.; Yu, W. *J. Am. Chem. Soc.* **1999**, *121*, 4316–4324.
- Kolano, C.; Helbing, J.; Bucher, G.; Sander, W.; Hamm, P. *J. Phys. Chem. B* **2007**, *111*, 11297–11302.
- Cummings, S. D.; Eisenberg, R. *J. Am. Chem. Soc.* **1996**, *118*, 1949–1960.
- Itoh, S.; Nagagawa, M.; Fukuzumi, S. *J. Am. Chem. Soc.* **2001**, *123*, 4087–4088.
- Weinstein, J. A.; Blake, A. J.; Davies, E. S.; Davis, A. L.; George, M. W.; Grills, D. C.; Lileev, I. V.; Maksimov, A. M.; Matousek, P.; Ya, M.; Parker, A. W.; Platonov, V. E.; Towrie, M.; Wilson, C.; Zheligovskaya, N. N. *Inorg. Chem.* **2003**, *42*, 7077–7085.
- Carles, S.; Lecomte, F.; Schermann, J.-P.; Desfrancois, C.; Xu, S.; Milles, J. M.; Bowen, K. H.; Bergès, J.; Houée-Levin, C. *J. Phys. Chem. A* **2001**, *105*, 5622–5626.
- Antonello, S.; Benassi, R.; Gavioli, G.; Taddei, F.; Maran, F. *J. Am. Chem. Soc.* **2002**, *124*, 7529–7538.
- Antonello, S.; Daasbjerg, K.; Jensen, H.; Taddei, F.; Maran, F. *J. Am. Chem. Soc.* **2003**, *125*, 14905–14916.
- Gill, P. M. W.; Radom, L. *J. Am. Chem. Soc.* **1987**, *110*, 4931–4941.
- Fourré, I.; Silvi, B. *Heterocycl. Chem.* **2007**, *18*, 135–160.
- Johnson, D. L.; Polyak, S. W.; Wallace, J. C.; Martin, L. L. *Lett. Pept. Sci.* **2003**, *10*, 495–500.
- Zubarev, R. A.; Kruger, N. A.; Fridriksson, E. K.; Lewis, M. A.; Horn, D. M.; Carpenter, B. K.; McLafferty, F. W. *J. Am. Chem. Soc.* **1999**, *121*, 2857–2862.
- Uggerud, E. *Int. J. Mass Spectrom.* **2004**, *234*, 45–50.
- Uggerud, E. *Int. J. Mass Spectrom.* **2004**, *235*, 279.
- Tung, T.-L.; Stone, J. A. *Can. J. Chem.* **1975**, *53*, 3153–3157.
- Klassen, N. V.; Armstrong, D. A.; Gillis, H. A. *Can. J. Chem.* **1972**, *50*, 2833–2840.
- Purdie, J. W.; Gillis, H. A.; Klassen, N. V. *Can. J. Chem.* **1973**, *51*, 3132–3142.
- Faraggi, M.; Klapper, M. H.; Dorfman, L. M. *Biophys. J.* **1978**, *24*, 307–317.
- Weik, M.; Ravelli, R. B.; Silman, I.; Sussman, J. L.; Gros, P.; Kroon, J. *Proc. Natl. Acad. Sci. U.S.A.* **2000**, *97*, 623–628.
- Weik, M.; Bergès, J.; Raves, M. L.; Gros, P.; McSweeney, S.; Silman, I.; Sussman, J. L.; Houée-Levin, C.; Ravelli, R. B. G. *J. Synchrotron Radiat.* **2002**, *9*, 342–346.
- Bergès, J.; Rickards, G.; Rauk, A.; Houée-Levin, C. *Chem. Phys. Lett.* **2006**, *421*, 63–67.
- Bergès, J.; Rickard, G. A.; Rauk, A.; Houée-Levin, C. *Chem. Phys. Lett.* **2008**, *454*, 118–123.
- Rickard, G. A.; Bergès, J.; Houée-Levin, C.; Rauk, A. *J. Phys. Chem. B* **2008**, *112*, 5774–5787.
- Dumont, E.; Loos, P.-F.; Assfeld, X. *Chem. Phys. Lett.* **2008**, *458*, 276–280.
- Ho, B. K.; Dill, K. A. *PLoS Comput. Biol.* **2006**, *2*, 228–237.
- Kolano, C.; Helbing, J.; Kozinski, M.; Sander, W.; Hamm, P. *Nature (London)* **2006**, *444*, 469–472.
- Coutsias, E. A.; Seok, C.; Jacobson, M. P.; Dill, K. A. *J. Comput. Chem.* **2004**, *25*, 510–528.
- Matthews, B. W.; Craik, C. S.; Neurath, H. *Proc. Natl. Acad. Sci. U.S.A.* **1994**, *91*, 4103–4105.
- Leduc, A.-M.; Trent, J. O.; Wittliff, J. L.; Bramlett, K. S.; Briggs, S. L.; Chirgadze, N. Y.; Wang, Y.; Burris, T. P.; Spatola, A. F. *Proc. Natl. Acad. Sci. U.S.A.* **2003**, *100*, 11273–11278.
- Moroder, L. *J. Pept. Sci.* **2005**, *11*, 258–261.
- Ainavarapu, S. R. K.; Wiita, A. P.; Huang, H. H.; Fernandez, J. M. *J. Am. Chem. Soc.* **2008**, *130*, 436–437.
- Angell, Y.; Chen, D.; Brahimi, F.; Saragovi, H. U.; Burgess, K. *J. Am. Chem. Soc.* **2008**, *130*, 556–565.
- Barret, G. C.; Elmore, D. T. *Amino Acids and Peptides*; Cambridge University Press: New York, 1998.
- Ranganathan, D.; Lakshmi, C.; Karle, I. L. *J. Am. Chem. Soc.* **1999**, *121*, 6103–6107.
- Wang, X.-Y.; Wang, Q.; Huang, X.-Y.; Wang, T.; Yu, X.-Q. *Arxiv* **2006**, *xi*, 148–154.
- Luscombe, N. M.; Austin, S. E.; Berman, H. M.; Thornton, J. N. *Genome Biology* **2000**, *1*, 1–37.
- Holmgren, A. *Trends Biochem. Sci.* **1981**, *6*, 26–28.
- Gross, E.; Sevier, C. S.; Vala, A.; Kaiser, C. A.; Fass, D. *Nat. Struct. Biol.* **2002**, *9*, 61–67.
- Sawicka, A.; Skurski, P.; Hudgins, R. R.; Simons, J. *J. Phys. Chem. B* **2004**, *107*, 13505–13511.
- Möller, C.; Plesset, M. S. *Phys. Rev.* **1934**, *46*, 618–622.
- Gruning, M.; Gritsenko, O. V.; van Gisbergen, S. J. A.; Baerends, E. J. *J. Phys. Chem. A* **2001**, *105*, 9211–9218.
- Wiberg, K. B.; Hterski, J. W. O. *J. Comput. Chem.* **1997**, *18*, 108–114.
- Mei, Y.; Wu, E. L.; Han, K. L.; Zhang, J. Z. H. *Int. J. Quantum Chem.* **2006**, *106*, 1267–1276.
- Stewart, J. P. P. *J. Comput. Chem.* **1989**, *9*, 209–220.
- Stewart, J. P. P. *J. Comput. Chem.* **1989**, *9*, 221–264.
- Vreven, T.; Morokuma, K. *J. Comput. Chem.* **2000**, *21*, 1419–1432.
- Rienstra-Kiracofe, J. C.; Tschumper, G. S.; Schaefer III, H. F.; Nand, S.; Ellison, G. B. *Chem. Rev.* **2002**, *102*, 231–282.
- Ferre, N.; Olivucci, M. *J. Mol. Struct.: THEOCHEM* **2003**, *632*, 71–82.
- Dumont, E.; Loos, P.-F.; Laurent, A. D.; Assfeld, X. *J. Chem. Theor. Comput.* **2008**, *4*, 1171–1173.
- Braida, B.; Hiberty, P. C. *J. Phys. Chem. A* **2003**, *107*, 4741–4747.
- Becke, A. D. *Phys. Rev. A* **1988**, *38*, 3098–3100.
- Lee, C.; Yang, Y.; Paar, R. G. *Phys. Rev. B* **1988**, *37*, 785–789.
- Frisch M. J.; et al. Gaussian 03, Revision C.02; Gaussian, Inc., Wallingford, CT, 2004.
- Schaftenaar, G.; Noordik, J. H. *J. Comput.-Aided Mol. Des.* **2000**, *14*, 123–134.
- Perczel, A.; Jakli, I.; Foxman, B. M.; Fasman, G. D. *Biopolymers* **1996**, *38*, 723–732.
- Mohle, K.; Gumann, M.; Hofmann, H.-J. *J. Comput. Chem.* **1997**, *18*, 1415–1430.
- Kabsch, W. *Acta Crystallogr.* **1978**, *A34*, 827–828.
- Humphrey, W.; Dalke, A.; Schulten, K. *J. Mol. Graphics* **1996**, *14*, 33–38.
- Zhang, R.; Snyder, G. H. *J. Biol. Chem.* **1989**, *264*, 18472–18479.
- Urry, D. W.; Ohnishi, M.; Walter, R. *Proc. Natl. Acad. Sci. U.S.A.* **1970**, *66*, 111–116.
- Kotelchuck, D.; Scheraga, H. A.; Walter, R. *Proc. Natl. Acad. Sci. U.S.A.* **1972**, *69*, 3629–3633.
- Mutter, M. *J. Am. Chem. Soc.* **1977**, *99*, 8307–8314.
- Becke, A. D. *J. Chem. Phys.* **1993**, *98*, 1372–1377.
- Braida, B.; Hiberty, P. C.; Savin, A. *J. Phys. Chem. A* **1998**, *102*, 7872–7877.
- Karle, I. L.; Kishore, R.; Raghobama, S.; Balaram, B. *J. Am. Chem. Soc.* **1988**, *110*, 1958–1963.
- Kolano, C.; Gomann, K.; Sander, W. *Eur. J. Org. Chem.* **2004**, *2004*, 4167–4176.
- Chivers, P. T.; Prehoda, K. E.; Raines, R. T. *Biochemistry* **1997**, *36*, 4061–4066.
- Huand, F.; Nau, W. M. *Angew. Chem., Int. Ed.* **2003**, *42*, 2269–2272.
- Rouhier, N.; Gelhaye, E.; Jacquot, J.-P. *FEBS Lett.* **2002**, *511*, 145–149.
- Bergès, J.; Kassab, E.; Conte, D.; Adjadj, E.; Houée-Levin, C. *J. Phys. Chem. A* **1997**, *101*, 7809–7817.
- Meraldi, J.-P.; Hruba, V. J.; Brewster, A. I. R. *Proc. Natl. Acad. Sci. U.S.A.* **1977**, *74*, 1373–1377.
- Dill, K. A.; Bromberg, S.; Yue, K.; Fiebig, K. M.; Yee, D. P.; Thomas, P. D.; Chan, H. S. *Protein Sci.* **1995**, *4*, 561–602.
- Martins-Costa, M. T. C.; Ruiz-Lopez, M. F. *Chem. Phys.* **2007**, *332*, 341–347.
- Loos, P.-F.; Assfeld, X. *AIP Conf. Proc.* **2007**, *963*, 308–315.
- Schwieters, C. D.; Clore, G. M. *J. Phys. Chem. B* **2007**, *112*, 6070–6073.
- Bodansky, M.; Stahl, G. L. *Proc. Natl. Acad. Sci. U.S.A.* **1974**, *71*, 2791–2794.
- Hall, D.; Lyons, P. J.; Pavitt, N.; Trezise, J. A. *J. Comput. Chem.* **1982**, *3*, 89–94.
- Ptak, M. *Biopolymers* **1973**, *12*, 1575–1589.
- Tonelli, A. E. *Biopolymers* **2004**, *17*, 1175–1179.
- He, H. T.; Gursoy, R. N.; Kupczyk-Subotkowska, L.; Tian, J.; Williams, T.; Sahaan, T. J. *J. Pharm. Sci.* **2006**, *95*, 2222–2234.
- (89) Solvation effects, in homo- or heterogeneous media, have also a role to play. We cannot technically investigate effects of solvation (dielectric constant  $\epsilon$  close to or higher than 4 for crystal proteins). Yet, a previous investigation on a system model has shown that solvation only has a shifting



effect due to the symmetric nature of the hemi-bonded radical anion.<sup>32,81</sup> This would tend to suggest that our results are essentially transferable to condensed phases, as relative electron affinities will essentially remain constant. Thus we consider gas phase properties in this study.

(90) Such a cut along a peptidic bond is not out of reach, as recent developments in LSCF/MM have achieved satisfactory results for a cut along a peptidic bond.<sup>82</sup>

(91) Another equivalent possibility is to report the number  $n'$  of atoms of the arc: this measure is more suitable for comparison with organic compounds.

(92) The key difference may lie in the shape of the arc connecting the two cysteines. Peptidic bonds tend to distort the structure of short cyclic peptides, which in turn adopts a near-ellipsoidal shape.<sup>83</sup> The latter might govern the final value of the interatomic distance. In the same way that a

slight compression of the three-electron, two-sulfur bond was reported (systems acting as molecular pincers),<sup>32</sup> systems presenting an horizontal stretching effect might result in a significant elongation.

(93) These are redox disulfide-exchange reactions with glutathione in aqueous media. The interested reader is referred to the original paper<sup>67</sup> for an exhaustive description of experimental conditions. Let us note that these measurements involve complex reactions—a proton transfer occurs in a second step. The first step is likely to be kinetically determinant.

(94) This would have the advantage to enable a discussion based on absolute electron affinities.

(95) A hairpin corresponds to the association of two antiparallel  $\beta$ -sheets, linked *solely* by hydrogen bonds (Trpzip 4 is the most popular example).

JP806465E